Advances in Computational Sciences and Technology
ISSN 0973-6107 Volume 10, Number 8 (2017) pp.2643-2662

http://www.ripublication.com

Slip Flow of Radiative Unsteady Boundary Layer Flow of Nanofluid Past a Stretching Sheet with Convective Boundary Condition

G. Radha[1], N. Bhaskar Reddy[1] and K. Gangadhar[2]

[1]Dept. of mathematics, S.V. University, Tirupati, A.P, India.

[2]Dept. of Mathematics, ANU Ongole Campus, Ongole-523001, A.P., India.

Abstract

In this paper the unsteady boundary layer flow of a nanofluid past a stretching sheet with a convective surface boundary condition and radiation are studied. Slip flow is also considered. This model is used for a nanofluid, which incorporates the effects of Brownian motion and thermophoresis. The resulting non-linear partial differential equations of the governing flow field are converted into a system of coupled non-linear ordinary differential equations by using suitable similarity transformations, and the resultant equations are then solved numerically by using Runge-Kutta fourth order method along with shooting technique. The influence of significant parameters on velocity, temperature, concentration, skin friction coefficient, Nusselt number and Sherwood number has been studied and numerical results are presented graphically and in tabular form.

Keywords: Boundary layer flow, stretching surface, convective boundary condition, Slip flow, Brownian motion and Thermophoresis.

1. INTRODUCTION:

The thermal conductivity of fluids plays an important role in the heat transfer. However, it is observed that enhancement of the thermal conductivity of poor heat

transfer fluids is possible in view of the addition of nanoparticles in the base fluids. The nano particles can be found in metals such as (Cu, Ag), oxides (Al_2O_3), carbides (SiC), nitrides (AiN, SiN) or nonmetals (graphite, carbon nanotubes). Nanofluids have novel properties that make them potentially useful in many applications in heat transfer including microelectronics, fuel cells, pharmaceutical processes and hybrid-powered engines. Nanoparticles provide a bridge between bulk materials and molecular structure. The term "nanofluid" was first introduced by Choi [1].The thermal conductivity of nanofluids depends on factors such as particle size, volume fraction of particles in the suspension and intrinsic thermal conductivities of the base fluid and particles. As a result many papers on nanofluids have been published, such as the papers by Xuan and Li [2], Xuan and Roetzel [3], Eastman et al. [4], Tiwari and Das [5] and Buongiorno [6]. In his paper, Buongiorno [6] developed an analytical model for convective transport in nanofluids which takes into account the Brownian diffusion and thermophoresis effects.

Convective boundary condition is mostly used to define a linear convective heat exchange condition for one or more algebraic entities in thermal. Heat transfer analysis with convective boundary conditions is evoked in processes such as thermal energy storage, gas turbines, nuclear plants, etc. In recent years, investigations on the boundary layer flow problem with a convective surface boundary condition have gained much interest among researchers, since first introduced by Aziz [7], who considered the thermal boundary layer flow over a flat plate in a uniform free stream with a convective surface boundary condition. Ishak [8] obtained the similarity solutions for the steady laminar boundary layer flow over a permeable plate with a convective boundary condition. Makinde and Aziz [9] investigated numerically the effect of a convective boundary condition on the two dimensional boundary layer flows past a stretching sheet in a nanofluid. Suneetha and Gangadhar [10] studied the thermal radiation effect on MHD stagnation point flow of a Carreau fluid with convective boundary condition.

The flow over a stretching surface is an important problem in many engineering processes with applications in industries such as extrusion, melt-spinning, the hot rolling, wire drawing, glass–fiber production, manufacture of plastic and rubber sheets, cooling of a large metallic plate in a bath, which may be an electrolyte, etc. In industry, polymer sheets and filaments are manufactured by continuous extrusion of the polymer from a die to a windup roller, which is located at a finite distance away. The thin polymer sheet constitutes a continuously moving surface with anon-uniform velocity through an ambient fluid by Takhar et al. [11]. Experiments show that the velocity of the stretching surface is approximately proportional to the distance from the orifice by Vleggaar [12]. The unsteady boundary layer flow over a stretching sheet has been studied by Devi et al. [13], Elbashbeshy and Bazid[14]and very recently by Ishak et al. [15]. Bala Anki Reddy and Suneetha [16] shed light on the boundary layer

flow of maxwell nano fluid over an exponentially stretching surface with aligned magnetic field and convective boundary condition.

Considerable interest has been shown on the boundary layer flow over a shrinking sheet in recent years. Some of the applications of the shrinking sheet problem in industry relate to the shrinking film that is can be unwrapped easily with adequate heat and used in the packaging of bulk products. The shrinking fluid flow study, which is essentially a backward flow, can also be applied to the study of hydraulic properties of agricultural clay soils, capillary effects in the shrinking-swell behaviour and small pores. The related changes in mechanical and hydraulic studies of such soils have a significant impact on the behaviour and the transport properties of the fluid. The fluid loses the memory of the perturbation produced by the slot for this backward flow configuration. Due this reason, the fluid flow due to a shrinking sheet has some quite distinct physical characteristics compared to the forward stretching case.

At high temperatures attained in some engineering devices, gas, for example, can be ionized and so becomes an electrical conductor. The ionized gas or plasma can be made to interact with the magnetic and alter heat transfer and friction characteristic. Since some fluids can also emit and absorb thermal radiation, it is of interest to study the effect of magnetic field on the temperature distribution and heat transfer when the fluid is not only an electrical conductor but also it is capable of emitting and absorbing thermal radiation. This is of interest because heat transfer by thermal radiation has become of greater importance when we are concerned with space applications and higher operating temperatures. Hady et al. [17] investigated the effects of thermal radiation on the viscous flow of a nanofluid and heat transfer over a non-linearly stretching sheet. Olanrewaju & Olanrewaju et al. [18] studied the boundary layer flow of nanofluids over a moving surface with radiation effects.

A slip flow model more accurately describes the non-equilibrium region near the interface. A partial slip may occur on a stationary and moving boundary when the fluid is particulate such as emulsions, suspensions, foams and polymer solutions. Beavers and Joseph [19] were the first to investigate the fluid flow at the interface between a porous medium and fluid layer in an experimental study and proposed a slip boundary conditions at the porous interface. In biomedical engineering, when blood flows through an artery slip flow is evident from experimental observations [20, 21]. The slip flows under different flow configurations have been studied in recent years [21–26]. Recently Rahman [27] studied combined effects of slip flow and convective surface heat flux on hydromagnetic boundary layer flow over a flat plate with variable fluid properties. Bala Anki Reddy et al. [28] investigated the numerical study of MHD boundary layer slip flow of a maxwell nanofluid over an exponentially stretching surface with convective boundary condition.

Motivated by the above-mentioned studies, this paper aims to study the two-

dimensional boundary layer flow of a nanofluid past a stretching sheet with convective boundary condition. Slip flow and radiation are also considered. The transformed governing equations are solved numerically via Runge–Kutta based shooting technique. The influence of dimensionless parameters on velocity, temperature and concentration profiles along with the friction factor, local Nusselt and Sherwood numbers are discussed with the help of graphs and tables.

2. MATHEMATICAL FORMULATION:

Consider an unsteady, two-dimensional (x, y) boundary layer flow of a viscous and incompressible fluid over a stretching/shrinking sheet immersed in a nanofluid. It is assumed that at time t =0, the velocity of the sheet is U_w $(x, t) = 0$. The unsteadiness in the flow field is caused by the time dependent velocity of the stretching sheet, which is given by $U_w = Ax/t$ where $A > 0$, $t > 0$. It is also assumed that the constant mass flux velocity is v_0 (x, t) with v_0 (x, t) < 0 for suction and v_0 (x, t) > 0 for injection or withdrawal of the fluid. The nanofluid is confined to $y > 0$, where y is the coordinate measured normal to the stretching surface as shown in Fig. 1. The governing equations for the steady conservation of mass, momentum, thermal energy and nanoparticle volume fraction equations can be written as [29]

$$\frac{\partial u}{\partial x}+\frac{\partial v}{\partial y}=0 \tag{1}$$

$$\frac{\partial u}{\partial t}+u\frac{\partial u}{\partial x}+v\frac{\partial u}{\partial y}=-\frac{1}{\rho_f}\frac{\partial P}{\partial x}+\omega\left(\frac{\partial^2 u}{\partial x^2}+\frac{\partial^2 u}{\partial y^2}\right) \tag{2}$$

$$\frac{\partial v}{\partial t}+u\frac{\partial v}{\partial x}+v\frac{\partial v}{\partial y}=-\frac{1}{\rho_f}\frac{\partial P}{\partial y}+\omega\left(\frac{\partial^2 v}{\partial x^2}+\frac{\partial^2 v}{\partial y^2}\right) \tag{3}$$

$$\begin{aligned}&\frac{\partial T}{\partial t}+u\frac{\partial T}{\partial x}+v\frac{\partial T}{\partial y}=\alpha\left(\frac{\partial^2 T}{\partial x^2}+\frac{\partial^2 T}{\partial y^2}\right)\\&+\tau\left\{D_B\left(\frac{\partial C}{\partial x}\frac{\partial T}{\partial x}+\frac{\partial C}{\partial y}\frac{\partial T}{\partial y}\right)+\frac{D_T}{T_\infty}\left[\left(\frac{\partial T}{\partial x}\right)^2+\left(\frac{\partial T}{\partial y}\right)^2\right]\right\}-\frac{1}{\rho C_p}\frac{\partial q_r}{\partial y}\end{aligned} \tag{4}$$

$$\frac{\partial C}{\partial t}+u\frac{\partial C}{\partial x}+v\frac{\partial C}{\partial y}=D_B\left(\frac{\partial^2 C}{\partial x^2}+\frac{\partial^2 C}{\partial y^2}\right)+\frac{D_T}{T_\infty}\left(\frac{\partial^2 T}{\partial x^2}+\frac{\partial^2 T}{\partial y^2}\right) \tag{5}$$

The radiative heat flux q_r is described by Rosseland approximation such that

$$q_r = -\frac{4\sigma^* \partial T^4}{3K' \partial y} \tag{6}$$

where σ^* and K' are the Stefan-Boltzmann constant and the mean absorption coefficient, respectively.

It should be noted that, by using the Rosseland approximation, the present analysis is limited to optically thick fluids. If the temperature differences within the flow are sufficiently small, then equation (6) can be linearized by expanding T^4 into the Taylor's series about T_∞, and neglecting higher order terms, we get

$$T^4 \cong 4T_\infty^3 T - 3T_\infty^4 . \tag{7}$$

Using equations (6) and (7) in equation (4), we obtain

$$\begin{aligned} &\frac{\partial T}{\partial t} + u\frac{\partial T}{\partial x} + v\frac{\partial T}{\partial y} = \alpha\left(1 + \frac{16\sigma^* T_\infty^3}{3K'k}\right)\left(\frac{\partial^2 T}{\partial x^2} + \frac{\partial^2 T}{\partial y^2}\right) \\ &+ \tau\left\{D_B\left(\frac{\partial C}{\partial x}\frac{\partial T}{\partial x} + \frac{\partial C}{\partial y}\frac{\partial T}{\partial y}\right) + \frac{D_T}{T_\infty}\left[\left(\frac{\partial T}{\partial x}\right)^2 + \left(\frac{\partial T}{\partial y}\right)^2\right]\right\} \end{aligned} \tag{8}$$

where u and v are the velocity components along the x - axis and y - axis, respectively, P is the fluid pressure, T is the fluid temperature, α is the thermal diffusivity, ω is the kinematic viscosity, D_B is the Brownian diffusion coefficient, D_T is the thermophoresis diffusion coefficient, $\tau = (\rho c)_p / (\rho c)_f$ is the ratio of the effective heat capacity of the particles to that of the fluid with ρ and c being the density and the specific heat at constant pressure, respectively, T is the temperature of the fluid, C is the concentration of the fluid, T_∞ is the ambient temperature, C_∞ is the ambient concentration, h is the wall heat transfer coefficient, k_m is the wall mass transfer coefficient, convective heat transfer processes is characterized by temperature T_f and associated concentration near the surface is C_f . The subscript ∞ represents the values at large values of y (outside the boundary layer). Details of the derivation of Eqs. (4) and (5) are given in the papers by Buongiorno [30] and Nield and Kuznetsov [31].

Eqs. (1) - (5) are subjected to the following boundary conditions [32, 33]:

$$\begin{aligned} &t = 0 : v(x,y,t) = 0,\ u(x,y,t) = 0,\ T(x,y,t) = T_w,\ C(x,y,t) = C_w \\ &t > 0 : v(x,t) = v_0(x,t), u(x,t) = U_w(x,t) + L\frac{\partial u}{\partial y}(x,t), \\ &-k\frac{\partial T}{\partial y} = h(T_f - T), -D_B\frac{\partial C}{\partial y} = k_m(C_f - C)\ at\ y = 0 \end{aligned} \tag{9}$$

$$u(x, y, t) \to 0 , v(x, y, t) \to 0 , T(x, y, t) \to T_\infty , \ C(x, y, t) \to C_\infty \text{ as } y \to \infty \tag{10}$$

k is the thermal conductivity of the base fluid, L is the slip length. The subscript w denotes the values at the solid surface. The governing Eqs. (1) – (5) subjected to the boundary conditions (9) and (10) can be expressed in a simpler form by introducing the following transformation:

$$\psi = Ax\left(\omega/t\right)^{1/2} f(\eta), \quad \eta = (\omega t)^{-1/2} y, \quad \theta(\eta) = \frac{T - T_\infty}{T_f - T_\infty}, \quad \phi(\eta) = \frac{C - C_\infty}{C_f - C_\infty} \tag{11}$$

Where η is the similarity variable and ψ is the stream function defined as u = ∂ψ / ∂y and

v =−∂ψ/∂x, which identically satisfies Eq. (1). By employing the boundary layer approximations and the similarity variables (11), Eqs (2), (3), (5) & (8) reduce to the following nonlinear ordinary differential equations:

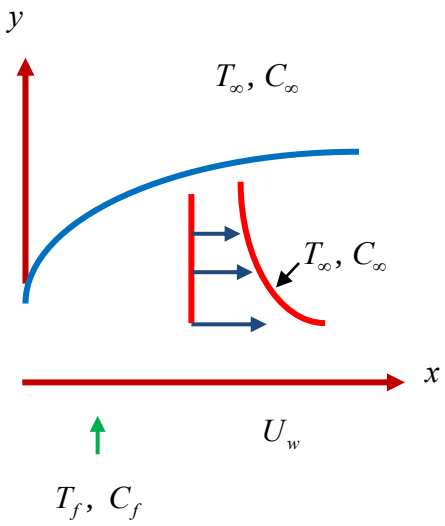

Fig .1 Geometry of the problem

$$f''' + A(ff'' - f'^2) + f' + \frac{\eta}{2} f'' = 0 \tag{12}$$

$$\frac{(1+R)}{p_r}\theta'' + \left(Af + \frac{\eta}{2}\right)\theta' + Nb\beta'\theta' + Nt\theta'^2 = 0, \tag{13}$$

$$\phi'' + \frac{Nt}{Nb}\theta'' + Le\left(Af + \frac{\eta}{2}\right)\phi' = 0 \tag{14}$$

and the boundary condition (9) and (10) become

$$f(0)=0, f'(0)=1+\alpha f''(0), \theta'(0)=-\beta_1\left[1-\theta(0)\right]; \phi'(0)=-\beta_2\left[1-\phi(0)\right]$$

(15)

$$f'=0=\theta=0, \phi=0 \ as \ \eta\to\infty \tag{16}$$

Where primes denote differentiation with respect to η. Further, *Pr* is the Prandtl number, *Nb* is the Brownian motion parameter, *Nt* is the thermophoresis parameter, R is the radiation parameter, *Le* is the Lewis number, α is velocity slip parameter, β_1 Thermal Biot number, β_2 concentration Biot number which are defined as

$$\Pr=\frac{\omega}{\alpha}, Nb=\frac{\tau D_B(C_w-C_\infty)}{\omega}, Nt=\frac{\tau D_T(T_f-T_\infty)}{T_\infty\omega}, Le=\frac{\omega}{D_B},$$

$$\alpha=L\sqrt{a/4}\ , \ R=\frac{16\sigma^* T_\infty^3}{3k^* v\rho c_p k_0}, \alpha=\frac{L}{(\omega t)^{1/2}}, \beta_1=\frac{h}{k}(\omega t)^{1/2}, \beta_2=\frac{k_m}{D_B}(\omega t)^{1/2} \tag{17}$$

Where we take $h=c/\sqrt{t}$, to obtain similarity solution. When *Nb* = *Nt* = 0, the present problem reduces to a regular viscous fluid, and the nanoparticle volume fraction Eq. (14) becomes ill posed and is of no physical significance.

The physical quantities of interest are the skin friction coefficient C_f, the local Nusselt number Nu_x and local Sherwood number Sh_x which are defined as

$$C_f=\frac{\tau_w}{\rho U_w^2}, \quad Nu_x=\frac{xq_w}{k(T_f-T_\infty)}, \qquad Sh_x=\frac{xq_m}{D(C_w-C_\infty)} \tag{18}$$

where τ_w, q_w and q_m are the surface shear stress and, heat and mass flux, respectively, which are given by [7]

$$\tau_w=\mu\left(\frac{\partial u}{\partial y}\right)_{y=0}, \ q_w=-k\left(\frac{\partial T}{\partial y}\right)_{y=0}, \ q_m=-D\left(\frac{\partial C}{\partial y}\right)_{y=0} \tag{19}$$

Using the similarity variables (11), we obtain

$$C_f \,\mathrm{Re}_x^{-1/2}=A^{-1/2}f''(0), \ Nu_x \,\mathrm{Re}_x^{-1/2}=-A^{-1/2}\theta'(0), \ Sh_x \,\mathrm{Re}_x^{-1/2}=-A^{-1/2}\phi'(0) \tag{20}$$

Where $\mathrm{Re}_x=\frac{xU_w}{\omega}$ is the local Reynolds number.

3. RESULTS AND DISCUSSIONS:

The system of coupled nonlinear differential equations (12) - (14) subject to the

boundary conditions (15)-(16) are solved numerically by using the Runge-Kutta algorithm with a systematic guessing of $f''(0), \theta'(0)$ and $\phi'(0)$ by the shooting method until the boundary conditions at infinity $f(0), \theta(0)$ and $\phi(0)$ decay exponentially to zero. In order to judge the validity and accuracy of this method, the obtained numerical solutions for the heat transfer coefficient are compared with the available literature and are found to be in good agreement, as shown in Table 1. In this study, the default values of the parameters are chosen as $R= 0.5, Pr=2, Le = 2, Nt = Nb = 0.1, \beta_1 =0.1, \beta_2 =0.2, \alpha = 0.5$ unless, otherwise specified.

Table 2 represents variation skin friction co-efficient for different values of α with $A=0$ and $A=2$. From table 2 we noticed that as α increase the skin friction decreases. Table 3 indicates that the Nusselt number $-\theta'(0)$ and Sherwood number $-\phi'(0)$ consistently lower for higher values of *Nb* and *Nt* for the both cases $A=0$ and $A=2$. As *Nb* increases the Nusselt number decreases and an opposite trend observed for Sherwood number. An increase β_1 increases the Nusselt number and decreases the Sherwood number .The Nusselt decreases as β_2 increases while Sherwood number increases as β_2 increases.

Fig.2 depicts the non-dimensional velocity for different values of slip parameter α, with acceleration parameter $A=0.0$ and $A=2.0$. It is observed that the velocity increases with increase in α for $A =0.0$. Whereas the velocity decreases with increase in α for $A=2.0$.

Fig. 3 depicts the influence of radiation parameter on temperature profiles of the flow. It is evident from the figure that an increase in the radiation parameter enhances the temperature profiles of the flow. Thermal radiation is responsible in thickening the thermal boundary layer at the expense of releasing heat energy from the flow region and it causes the system to cool. In reality this is true because temperature increases as a result of increasing the Rosseland diffusion approximation for radiation q_r.

The effect of thermophoresis parameter *Nt* on the temperature distribution is demonstrated in Fig.4. It is clearly shown that an increase in the thermophoresis parameter leads to increase the temperature for both cases $A=0.0$ and $A=2.0$. Fig.5 illustrates the variation of concentration with thermophoresis parameter. The concentration of the boundary layer increases with the increase in the thermophoresis parameter for both cases.

Fig.6 illustrates the variation of temperature with Brownian motion parameter *Nb*. This is due to fact that the Brownian motion generates micro-mixing which enhances the thermal conductivity of the nanofluid. This higher nanofluid thermal conductivity in effect causes the increase of temperature. The temperature in the boundary layer increases with the increase in the Brownian motion parameter for both cases. The effect of Brownian motion parameter on the concentration distribution is demonstrated in Fig.7. It is found that the concentration decreases as the Brownian

motion parameter increases for both the cases.

Figs. 8 and 9 illustrate the effect of thermal Biot number β_1 on the temperature and concentration profiles. It is verified that the temperature and concentration increases as the thermal Biot number increases. Figs.10 and 11 displays the variation of temperature and concentration profiles with respect to concentration Biot number β_2. It is noted that the temperature and concentration increases as the concentration Biot number increases.

Fig.12 illuminates a very important effect of Prandtl number on the temperature profile. An increase in Prandtl number reduces the temperature and the thermal boundary layer thickness for both cases. This is due to increase in Prandtl number the thermal conductivity of the fluid reduces and consequently, thermal boundary layer thickness decreases. Fig.13 displays the effect of Prandtl number on the concentration profile with. An increase in Prandtl number reduces the concentration.

Effects of regular Lewis number on solute concentration profile is shown in Fig.14. It is clearly shown that this parameter reduces the solute concentration profiles. By definition, regular Lewis number is a dimensionless number which is the ratio of thermal diffusivity to mass diffusivity. Increasing the value of *Le* is the same as maximizing thermal boundary layer thickness at the expense of minimizing solutal boundary layer thickness which increases mass transfer rate.

Table 1. Comparison of $-f''(0)$ with the available results in literature for different values of α when $A = 1$.

α	$-f''(0)$		
	Andersson [34]	Mahmoud [35]	Present study
0	1.0000	1.00000	1.000000
0.1	0.8721	0.87208	0.872083
0.2	0.77640	0.77637	0.776377
0.5	0.5912	0.59190	0.591196
1.0	0.4302	0.43016	0.430160
2.0	0.2840	0.28398	0.283981
5.0	0.1448	0.14484	0.144842
10.0	0.0812	0.08124	0.081245
20.0	0.0438	0.04378	0.043792
50.0	0.0186	0.01859	0.018600
100.0	0.0095	0.00955	0.009553

Table 2. Values of $-f''(0)$ for different α when $A=0$ and $A=2$.

$-f''(0)$

α	$A=0$	$A=2$
0.1	10.0640421862	0.9793458716
0.5	2.0006385600	0.6127243015
1.0	1.0000015635	0.4271293119
1.5	0.6666666697	0.3308382027
2.0	0.5000000017	0.2711276919

Table 3 Variation of local Nusselt number and Sherwood number for different values of Nt, Nb, β_1 and β_2.

Nt	Nb	β_1	β_2	$-\theta'(0)$		$-\phi'(0)$	
				$A=0$	$A=2$	$A=0$	$A=2$
0.1	0.1	0.1	0.1	0.0864954156	0.0917317253	0.0893300067	0.0935946156
0.3	0.1	0.1	0.1	0.0862633470	0.0916378119	0.0844502487	0.0901473826
0.5	0.1	0.1	0.1	0.0860244463	0.0915419153	0.0798140796	0.0867758207
0.7	0.1	0.1	0.1	0.0857784016	0.0914439671	0.0754282233	0.0834814131
0.1	0.3	0.1	0.1	0.0863241403	0.0916672125	0.0910328367	0.0947673277
0.1	0.5	0.1	0.1	0.0861504994	0.0916021293	0.0913735116	0.0950018908
0.1	0.7	0.1	0.1	0.0859744674	0.0915364713	0.0915195934	0.0951024328
0.1	0.1	0.5	0.1	0.2780890306	0.3428484315	0.0839170776	0.0888862944
0.1	0.1	1.0	0.1	0.3823372645	0.5187158300	0.0810848968	0.0856661010
0.1	0.1	1.5	0.1	0.4362166765	0.6244881634	0.0796532552	0.0837607546
0.1	0.1	2.0	0.1	0.4690218833	0.6948172200	0.0787924788	0.0825071292
0.1	0.1	0.1	0.5	0.0862638530	0.0916296303	0.3371890249	0.3946302380
0.1	0.1	0.1	1.0	0.0860938919	0.0915384582	0.5162387246	0.6599703876
0.1	0.1	0.1	1.5	0.0859873300	0.0914722597	0.6272680502	0.8506160569
0.1	0.1	0.1	2.0	0.0859143016	0.0914220118	0.7028513048	0.9942163450

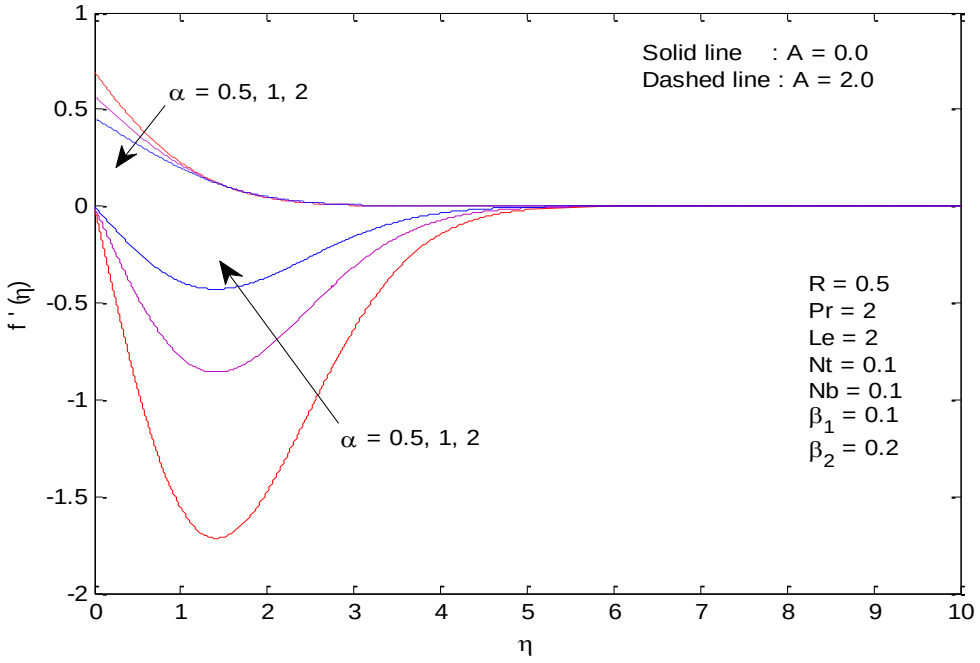

Fig 2: Effect of slip parameter on velocity profile.

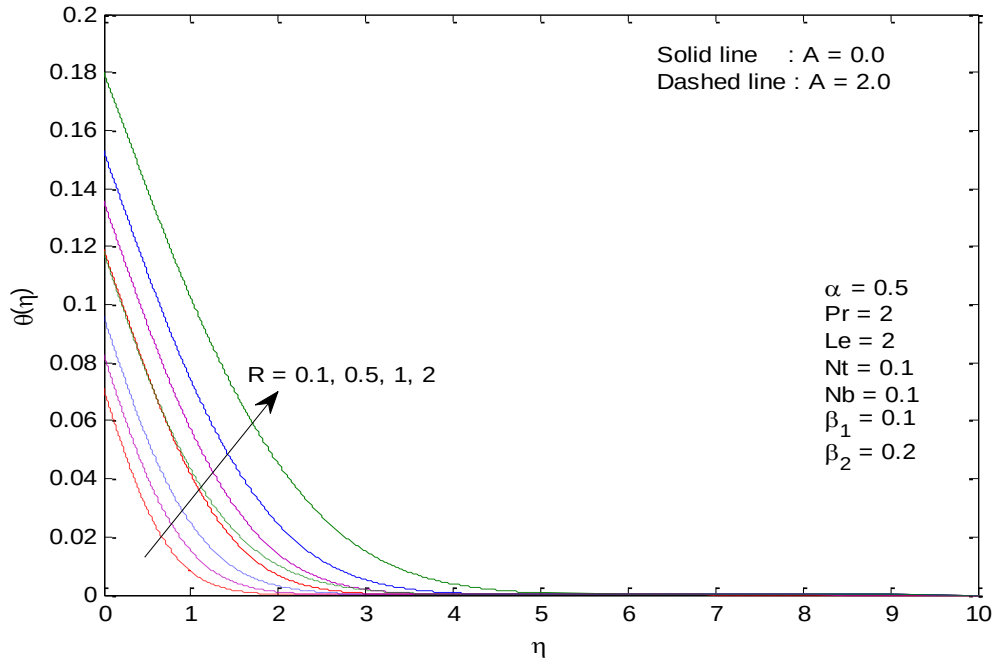

Fig.3: Effect of radiation parameter on temperature profile.

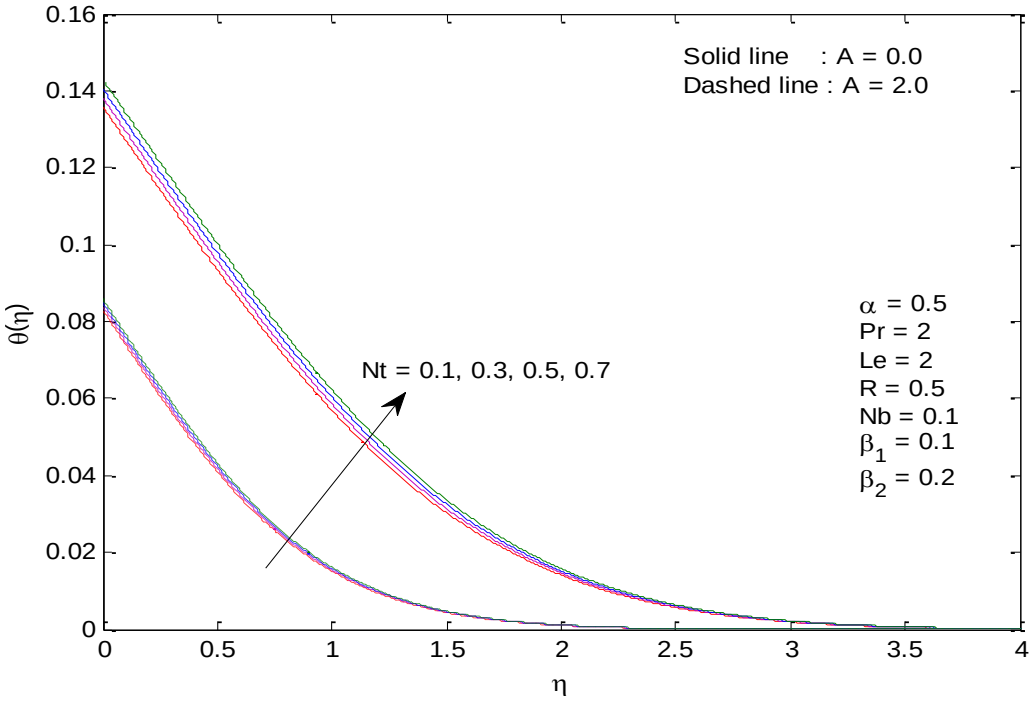

Fig.4: Effect of thermophoresis parameter on temperature profile.

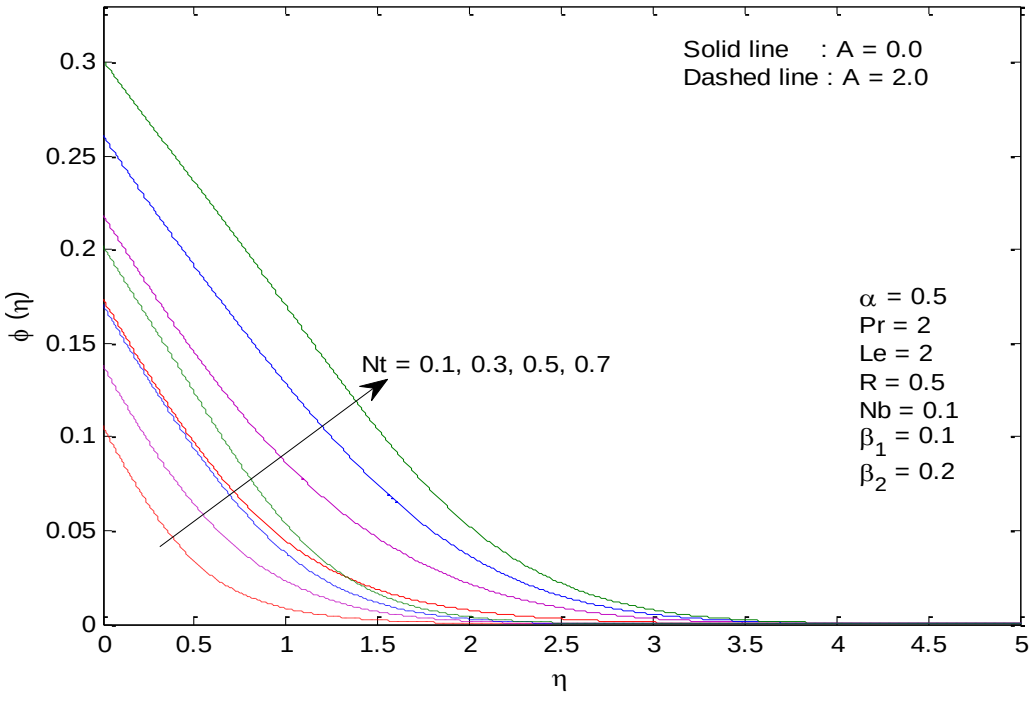

Fig.5: Effect of thermophoresis parameter on concentration profile.

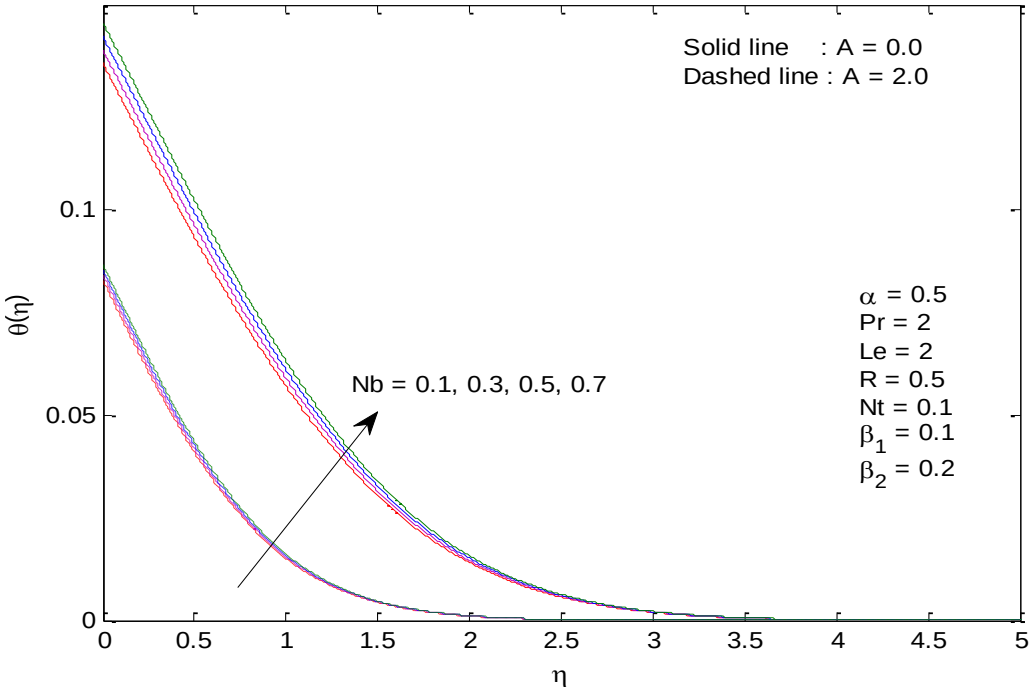

Fig.6: Effect of Brownian motion on temperature profile.

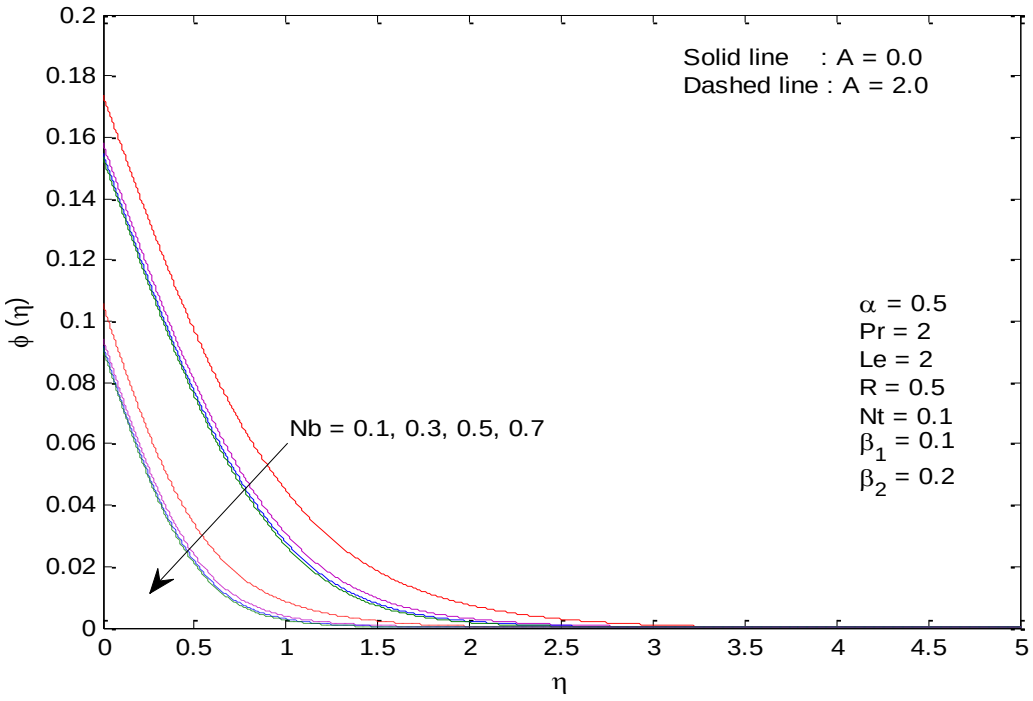

Fig.7: Effect of Brownian motion on concentration profile.

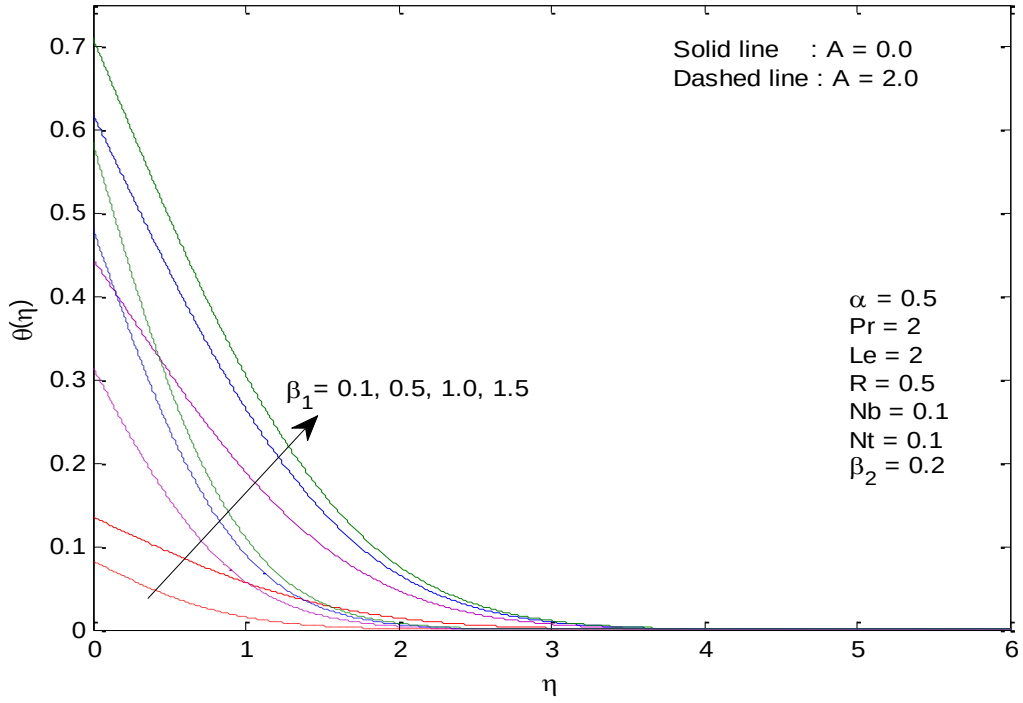

Fig.8: Effect of thermal Biot number on temperature profile.

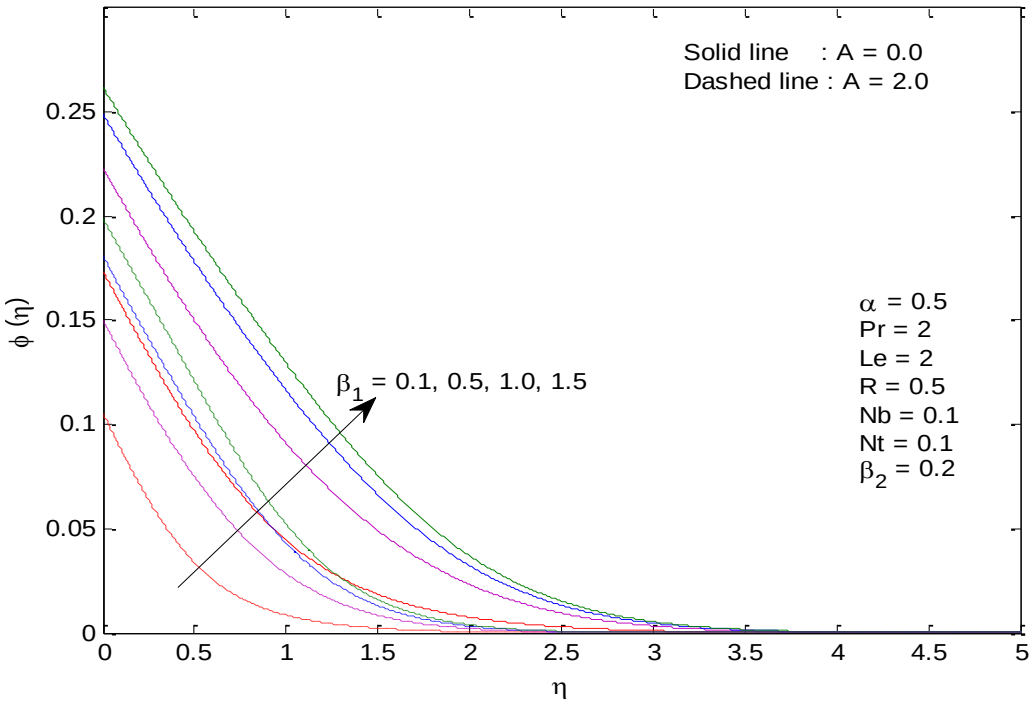

Fig.9: Effect of thermal Biot number on concentration profile.

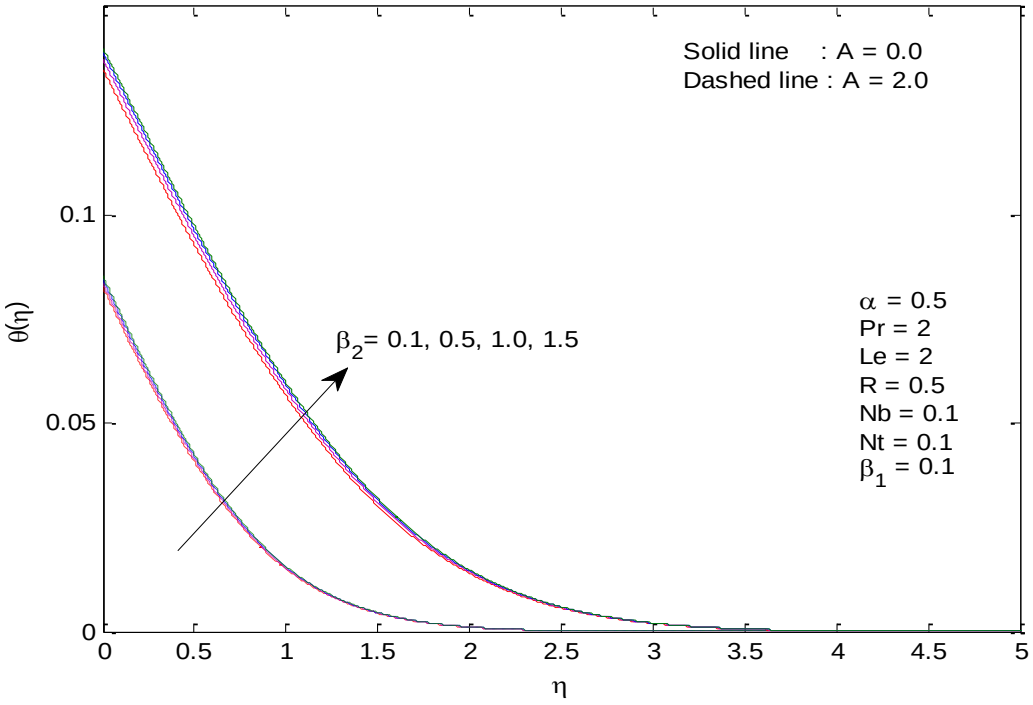

Fig.10: Effect of concentration Biot number on temperature profile.

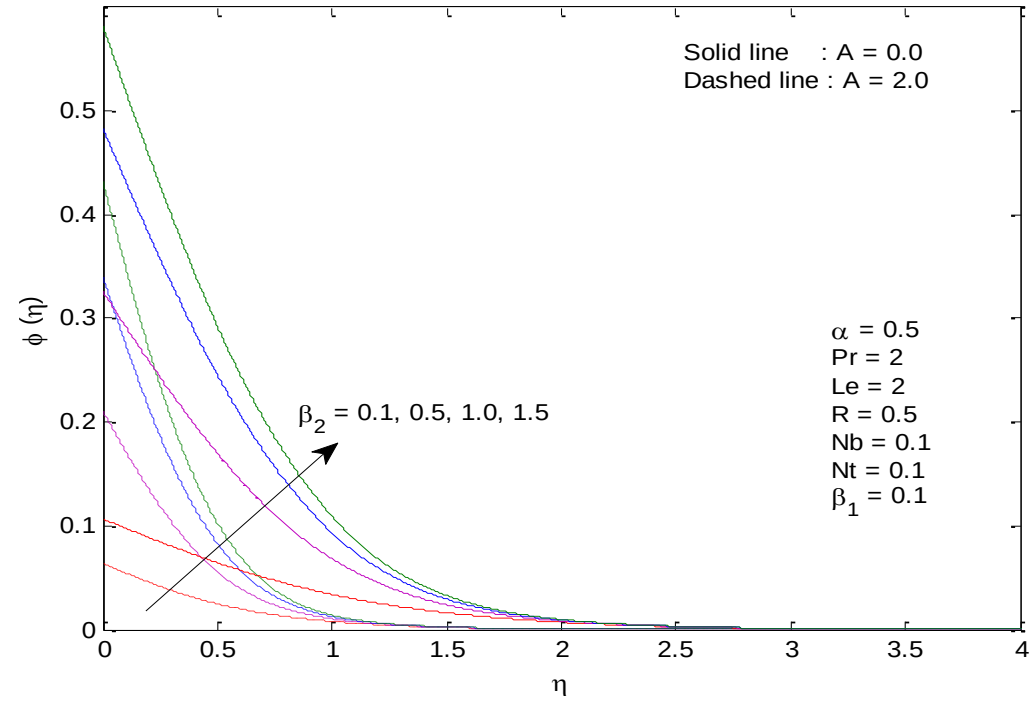

Fig.11: Effect of concentration Biot number on concentration profile.

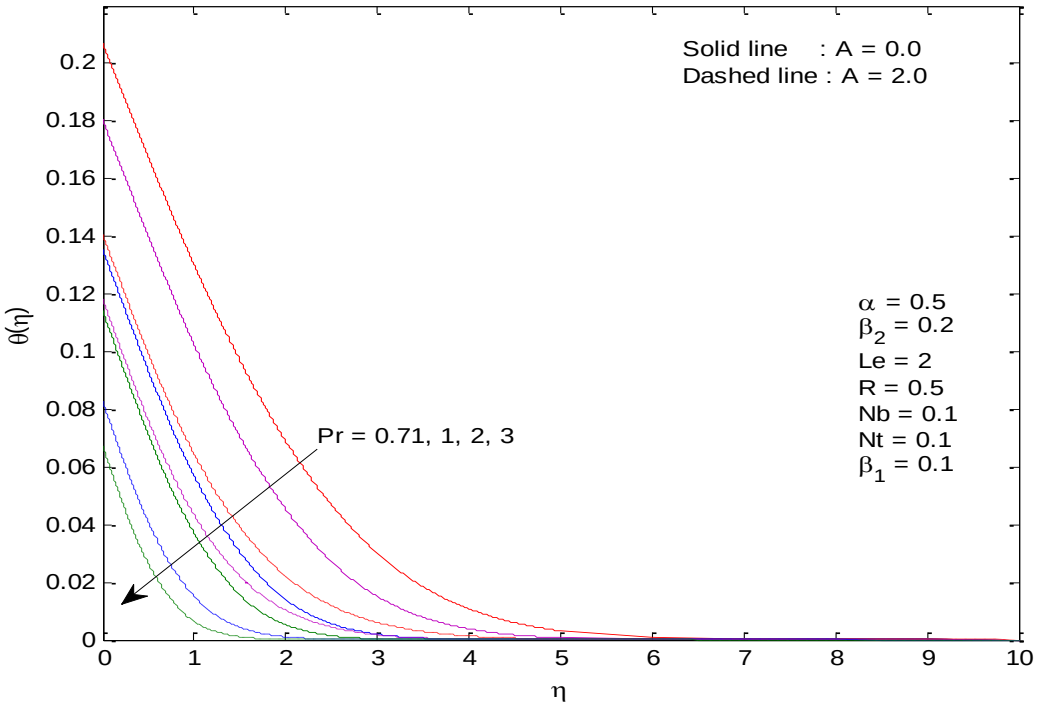

Fig.12: Effect of Prandtl number on temperature profile.

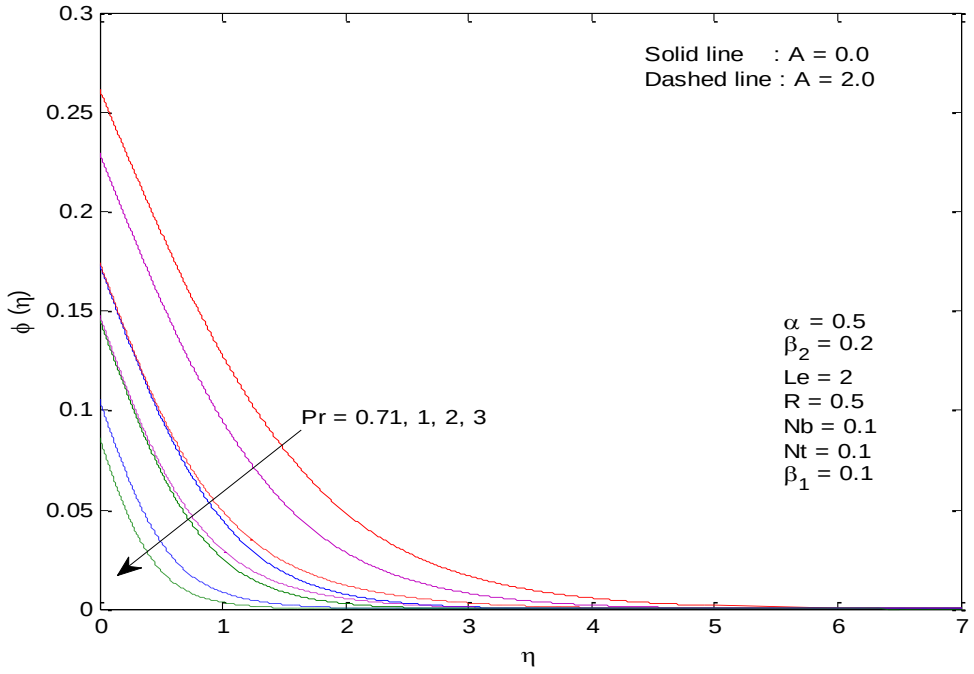

Fig.13: Effect of Prandtl number on concentration profile.

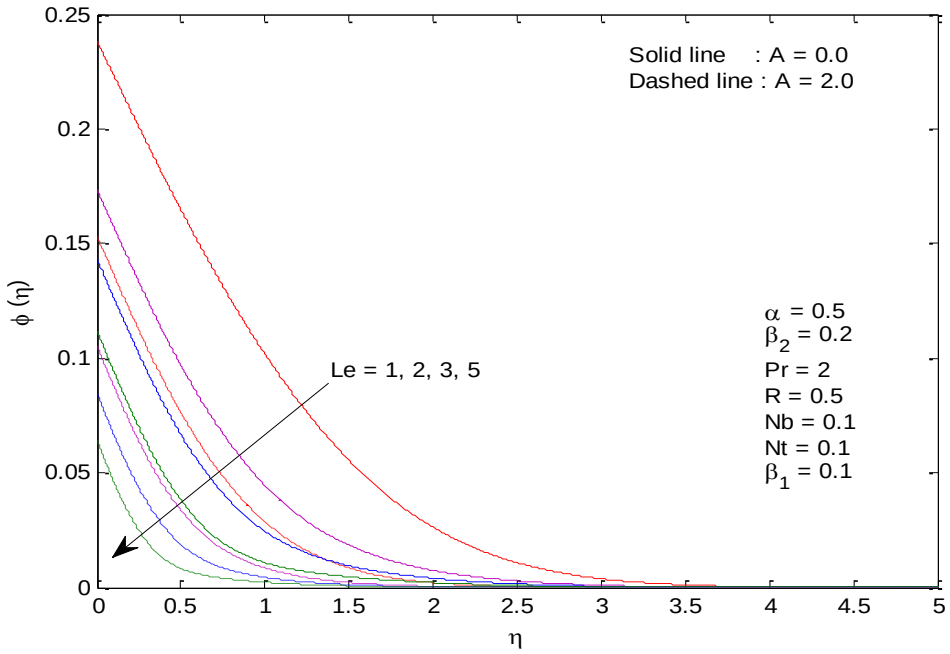

Fig.14: Effect of Lewis on concentration profile.

4. CONCLUSIONS

The unsteady boundary layer flow of a nanofluid past a stretching sheet with a convective boundary condition was studied. The effects of the acceleration parameter, thermal and concentration Biot numbers, Brownian motion parameter and thermophoresis parameter on the local Nusselt number and Sherwood numbers were studied. Numerical solutions to the governing equations were obtained using a shooting method. The results for the local Nusselt number are presented for different values of the governing parameters. An increase in the radiation parameter enhances the temperature profiles of the flow. Temperature and concentration increases as the thermal and concentration Biot numbers increases. It is also consistently higher for higher values of the convective parameter but lower for higher values of the acceleration parameter, Brownian motion parameter and thermophoresis parameter.

REFERENCES

[1] S. Choi, Enhancing thermal conductivity of fluids with nanoparticle, in Developments and Applications of Non-Newtonian Flows, A. Siginerand P.H.Wang, Eds., 66 (1995), 99–105, ASME, New York, NY,USA.(Book)

[2] Y. Xuan, Q. Li, Heat transfer enhancement of nanofluids, Int. J. Heat Fluid

Flow, 21 (2000), 58–64.

[3] Y. Xuan, W. Roetzel, Conceptions for heat transfer correlation of nanofluids, Int. J. Heat Mass Transf., 43 (2000), 3701–3707.

[4] J.A. Eastman, S.U.S. Choi, S. Li, W. Yu, L.J. Thompson, Anoma- lously increased effective thermal conductivities of ethylene glycol - based nanofluids containing copper nanoparticles, Appl. Phys. Lett., 78 (2001), 718–720.

[5] R.K. Tiwari, M.K. Das, Heat transfer augmentation in a two-sided lid-driven differentially heated square cavity utilizing nanofluids, Int. J. Heat Mass Transf., 50 (2007), 2002–2018.

[6] J. Buongiorno, Convective transport in nanofluids, J. Heat Transf., 128 (2006), 240–250.

[7] A. Aziz, A similarity Solution for Laminar Thermal Boundary Layer over a Flat Plate with a Convective Surface Boundary Condition, Commun. Nonlinear Sci. Numer. Simulat., 14 (2009), 1064-1068.

[8] A. Ishak, Similarity solutions for flow and heat transfer over a permeable surface with convective boundary condition, Appl. Math. Computation, 217(2010), 837-842. (periodical)

[9] O.D. Makinde and A. Aziz, Boundary Layer Flow of a Nanofluid Past a Stretching Sheet with Convective Boundary Condition, Int. J. Therm. Sci., 50 (2011), 1326-1332. (periodical)

[10] S. Suneetha and K. Gangadhar, Thermal Radiation Effect on MHD Stagnation Point Flow of a Carreau Fluid with Convective Boundary Condition, Open Science Journal of Mathematics and Application, 3(5): 121-127, 2015.

[11] H.S. Takhar, A.J. Chamkha, G. Nath, Unsteady three-dimensional MHD-boundary-layer flow due to the impulsive motion of a stretching surface, Acta Mech. 146 (2001), 59–71.

[12] J. Vleggaar, Laminar boundary layer behaviour on continuous accelerating surface, Chem. Eng. Sci., 32 (1977), 1517–1525.

[13] C. D. S. Devi, H. S. Takhar, G. Nath, Unsteady mixed convection flow in stagnation region adjacent to a vertical surface, HeatMassTransfer, 26(1991), 71–79.

[14] E. M. A. Elbashbeshy, M. A. A. Bazid, Heat transfer over an unsteady stretching surface, HeatMassTransfer, 41(2004), 1–4.

[15] A. Ishak, R. Nazar, I. Pop, Heat transfer over an unsteady stretching surface with prescribed heat flux, Can.J.Phys., 86(2008), 853–855.

[16] P. Bala Anki Reddy and S. Suneetha**,** Boundary layer flow of maxwell nano fluid over an exponentially stretching surface with alligned magnetic field and convective boundary condition, Global journal of pure and applied mathematics (GJPAM), Vol.12(3), 2016, 119-123.

[17] F. M. Hady, F. S. Ibrahim, S. M. Abdel-Gaiedand and M. R. Eid, Radiation effect on viscous flow of a nanofluid and heat transfer over a nonlinearly stretching sheet, Nanoscale Research Letters, 2012, 7:229.

[18] P.O. Olanrewaju, M. A. Olanrewaju and A.O. Adesanya, Boundary layer flow of nanofluids over a moving surface with radiation effects, International Journal of Applied Science and Technology, Vol. 2(1) 2012, 274-285.

[19] G. S. Beavers and D.D. Joseph, Boundary condition at a naturally permeable wall, J Fluid Mech., 30(1967),197–207.

[20] G. Bugliarello and J.W. Hayden, High speed microcinemato-graphic studies of blood flow in vitro. Science, 138(1962), 981–983.

[21] Y. Nubar, Blood flow, slip and viscometry, Biophys J., 11(1971), 252–264.

[22] T. Fang and C.F. Lee, Exact solutions of incompressible Couette flow with porous walls for slightly rarefied gases, Heat MassTransfer, 42(2006), 255–262.

[23] T. Fang, J. Zhang and S. Yao, (2009) Slip MHD viscous flow over a stretching sheet an exact solution, Commun Nonlinear Sci Numer Simul., 14(2009), 3731–3737.

[24] C.Y. Wang, Stagnation slip flow and heat transfer on a moving plate, Chem Eng Sci., 61(2006), 7668- 7672.

[25] C.Y. Wang, Stagnation flow on a cylinder with partial slip an exact solution of the Navier-Stokes equations, IMA J ApplMath., 72(2007), 271–277.

[26] C. Y. Wang, Analysis of viscous flow due to a stretching sheet with surface slip and suction, Nonlinear Anal Real World Appl., 10(2009), 375–380.

[27] M.M. Rahman, Locally similar solutions for Hydromagnetic and thermal slip flow Boundary layers over a flat plate with variable fluid properties and convective surface boundary condition, Meccanica, 46(5), 2011, 1127-1143.

[28] P. Bala Anki Reddy, S. Suneetha and N. Bhaskar Reddy, Numerical Study of MHD Boundary Layer Slip Flow of a Maxwell Nanofluid over an exponentially stretching surface with convective boundary condition, Propulsion and Power Research (2016) (accepted).

[29] M. Miklavčič and C.Y. Wang, Viscous flow due a shrinking sheet, Q Appl Math., 64 (2006), 283–290

[30] J. Buongiorno, Convective transport in nanofluids, J. Heat Transf., 128 (2006), 240–250.

[31] D.A. Nield and A.V. Kuznetsov, Thermal instability in a porous medium layer saturated by a nanofluid, Int. J. Heat Mass Transf., 52 (2009), 5796–5801.

[32] N. Bachok, A. Ishak and I. Pop, Unsteady boundary-layer flow and heat transfer of a nanofluid over a permeable stretching/shrinking sheet, Int. J. Heat Mass Transf., 55 (2012), 2102–210.

[33] T. Fang , J. Zhang , S. Yao , Viscous flow over an unsteady shrinking sheet with mass transfer, Chin. Phys. Lett. 26 (2009) 014703 .

[34] Andersson H.I., (2002), Slip flow past a stretching surface, Acta Mech., Vol.158, pp.121–125.

[35] Mahmoud, M.A.A., (2010), Chemical reaction and variable viscosity effects on flow and mass transfer of a non-Newtonian viscoelastic fluid past a stretching surface embedded in a porous medium, Meccanica, Vol.45, pp.835–846.